Electronic Supplementary Material (ESI) for Dalton Transactions. This journal is © The Royal Society of Chemistry 2022

Supporting Information

cis-Dipyridyl Porphyrin-Based Multicomponent Organoplatinum(II) Bismetallacycles for Photocatalytic Oxidation

Ying Cheng, [ab] Zeyuan Zhang,[ab] Xianglong Duan[*a] and Mingming Zhang[*ab]

[a.] Second Department of General Surgery, Shaanxi Provincial People's Hospital and Third Affiliated Hospital of Xi'an Jiaotong University, Xi'an 710068, P. R. China. E-mail: duanxianglong@nwpu.edu.cn, mingming.zhang@xjtu.edu.cn
[b.] State Key Laboratory for Mechanical Behavior of Materials, Shaanxi International Research Center for Soft Matter, School of Materials Science and Engineering, Xi'an Jiaotong University, Xi'an 710049, P. R. China

Table of Contents

1. Materials and methods

All reagents and deuterated solvents were used as purchased without further purification. Ligand **1**[S1] was prepared according to the literature procedures. Ligands **3a−c** were purchased in the carboxylic acid form and obtained by neutralization reaction with NaOH. NMR spectra were recorded on a Bruker Avance 600 MHz spectrometer. ^{1}H NMR chemical shifts were recorded relative to residual solvent signals. ^{31}P{^{1}H} NMR chemical shifts were referenced to an external unlocked sample of 85% H_3PO_4 (δ 0.0). Mass spectra were recorded on a Micromass Quattro II triple-quadrupole mass spectrometer using electrospray ionization with a MassLynx operating system. The UV/vis experiments were conducted on a Lambd 950 absorption spectrophotometer. The fluorescent experiments were conducted on a Hitachi F-7000 fluorescence spectrophotometer. X-ray diffraction analysis was conducted a Bruker D8 VENTURE PHOTON II MetalJet, in which crystals were frozen in paratone oil inside a cryoloop under a cold stream of N_2. The radiation monochromator Helios Multi-layer Optic was used for the structures. An empirical absorption correction using SADABS was applied for all data. The structures were solved and refined to convergence on F^2 for all independent reflections by the full-matrix least squares method using the OLEX2 1.2.

Singlet oxygen quantum yield measurements

Singlet oxygen generation studies were performed in DMSO using a LED lamp (λ_{ex} = 405 nm) as the light source. Before the experiment, the absorption of the photosensitizers, including ligand **1**, bismetallacycles **4a**, **4b**, and **4c**, at the excitation wavelength of 405 nm was kept as ca. 0.26. Quantum yields for singlet oxygen generation were determined by monitoring the decrease in the absorption of 1,3-diphenylisobenzofuran (DPBF) at 418 nm caused by its photooxidation sensitized. The time-dependent absorption spectra of DPBF were recorded per 1.0 min for homogeneous phase, respectively. The quantum yields of singlet oxygen generation ($^{1}O_2$) were calculated by using a relative method with optically matched solutions and by comparing the decrease in the absorbance of DPBF that was sensitized by photosensitizers as compared to 5,10,15,20-tetraphenylporphyrin (TPP) (Φ_Δ = 0.64) as a reference according to the equation:

$$\Phi_\Delta^{S} = \Phi_\Delta^{TPP} \frac{m^{S}F^{TPP}}{m^{TPP}F^{S}}$$

where superscripts "S" and "TPP" denote the photosensitizers and TPP, respectively, "Φ_Δ" is the quantum yield of singlet oxygen, "m" is the slope of a plot with a difference in the change in the absorbance of DPBF (at 418 nm) with the irradiation time, and "F" is the absorption correction factor, which is given by $F=1-10^{-OD}$ (OD corresponds to the absorbance of the photosensitizer).

Photooxidation of methyl(phenyl)sulfane (MPS)

MPS (26 μmol) and photosensitizers **1**, **4a**, **4b**, **4c** or TPP (1 mol%) were dissolved

in 2 ml DMSO-d_6 in a 5 mL glass vessel. Before the reaction, oxygen was bubbled into the reaction system for 5 min. The reaction vessel was then irradiated with a LED light (λ_{ex} = 405 nm, 4.36 W) at room temperature for corresponding time. The conversion was determined by ^{1}H NMR spectroscopy. Turnover frequency (TOF) of MPS photooxidation to sulfoxide by 1 mol% ligand **1**, **4a**, **4b**, and **4c** were calculated to describe the intrinsic catalytic activity of the photosensitizers according to the equation: TOF = (moles of substrate converted to the target product in the reaction) / (moles of active sites of catalysts in the reaction) / (reaction time).

2. Synthetic procedures and characterization data

*2.1 Synthesis of ligand **1***

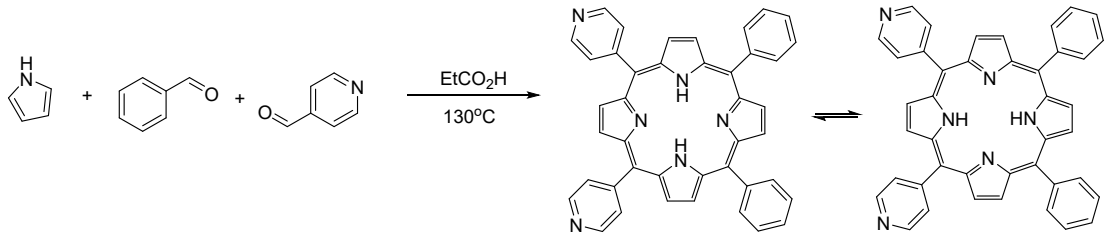

A solution of benzaldehyde (1.19 g, 11.18 mmol), 4-pyridinecarbaldehyde (1.20 g, 11.18 mmol), and pyrrole (1.50 g, 22.36 mmol) was heated at reflux (130°C) in propionic acid (150 mL) for 1 h. After being cooled to room temperature, the remaining solution was neutralized using aqueous NaOH solution, and the product was extracted with chloroform. The crude product of a mixture of six porphyrins was obtained by evaporating the solvent under reduced pressure. The targeted product was separated by using a dichloromethane/methanol solvent system consisting initially of 100% CH_2Cl_2, and gradually ending with 90% CH_2Cl_2: 10% CH_3OH. After separation, the desired product ligand **1** was collected as a purple red solid (668 mg, 9.7%). ^{1}H NMR (400 MHz, $CDCl_3$) δ 9.05 (d, J = 5.7 Hz, 1H), 8.91 (d, J = 4.8 Hz, 1H), 8.87 (s, 1H), 8.84 (s, 1H), 8.80 (d, J = 4.7 Hz, 1H), 8.21 (d, J = 6.2 Hz, 1H), 8.17 (d, J = 5.7 Hz, 1H), 7.79 (t, J = 8.2 Hz, 2H), -2.84 (s, 1H). The ^{1}H NMR spectra of ligand **1** matched with reported data.[S1]

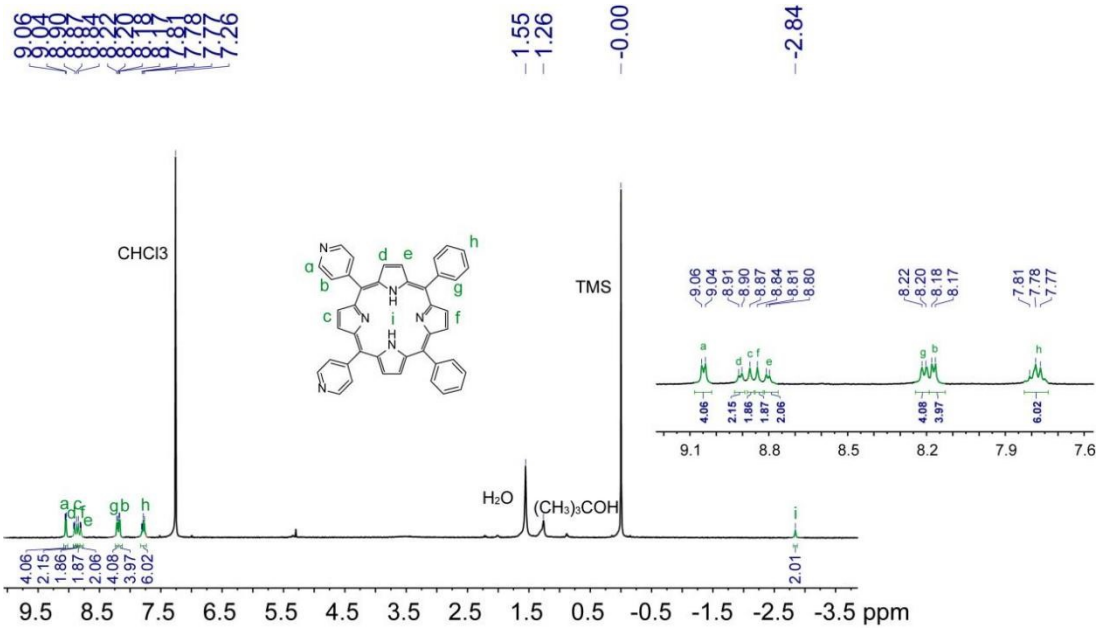

Figure S1. ^{1}H NMR spectrum (400 MHz, $CDCl_3$, 295 K) recorded for ligand **1**.

*2.2 Synthesis of ligand **3a–c***

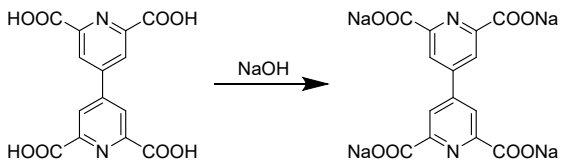

4,4-Bipyridine-2,2',6,6'-tetracarboxylic acid (100 mg, 0.30 mmol) and NaOH (51.3 mg, 1.28 mmol) were added in H_2O (50 mL) and stirred at room temperature for 3h. Then the mixture was concentrated and washed by acetone to give **3a** (120.1 mg, 95%) as a light green solid. ^{1}H NMR (600 MHz, CD_3OD) δ 4.80 (s, 1H).

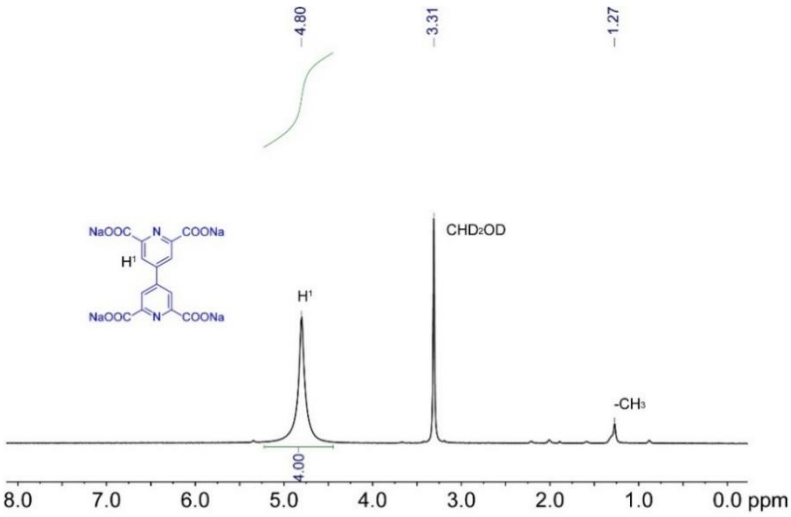

Figure S2. ^{1}H NMR spectrum (600 MHz, CD_3OD, 295 K) recorded for ligand **3a**.

Ligand **3b–c** were synthesized using the same method described above. **3b**, ^{1}H NMR (600 MHz, CD_3OD) δ 8.42 (t, J = 1.5 Hz, 1H), 8.14 (d, J = 1.5 Hz, 2H). **3c**, ^{1}H NMR (600 MHz, CD_3OD) δ 8.42 (t, J = 1.5 Hz, 1H), 8.36 (d, J = 1.5 Hz, 2H), 7.86 (s, 2H).

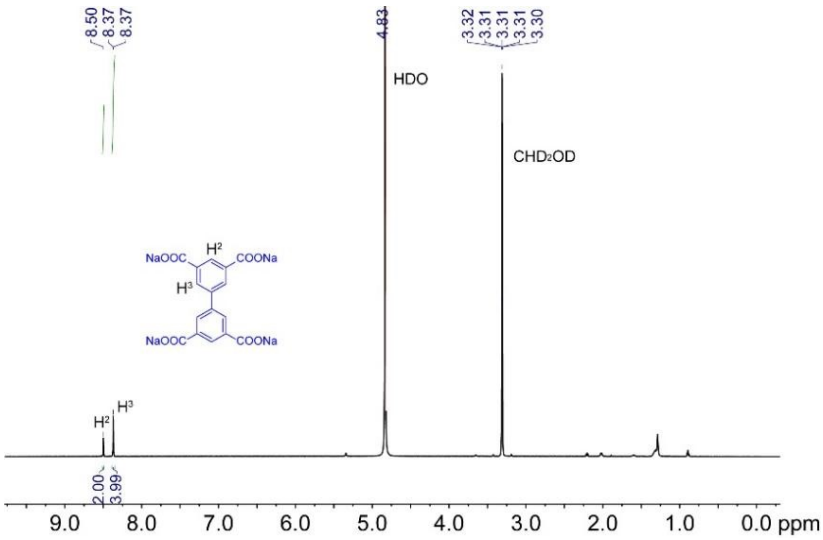

Figure S3. ^{1}H NMR spectrum (600 MHz, CD_3OD, 295 K) recorded for ligand **3b**.

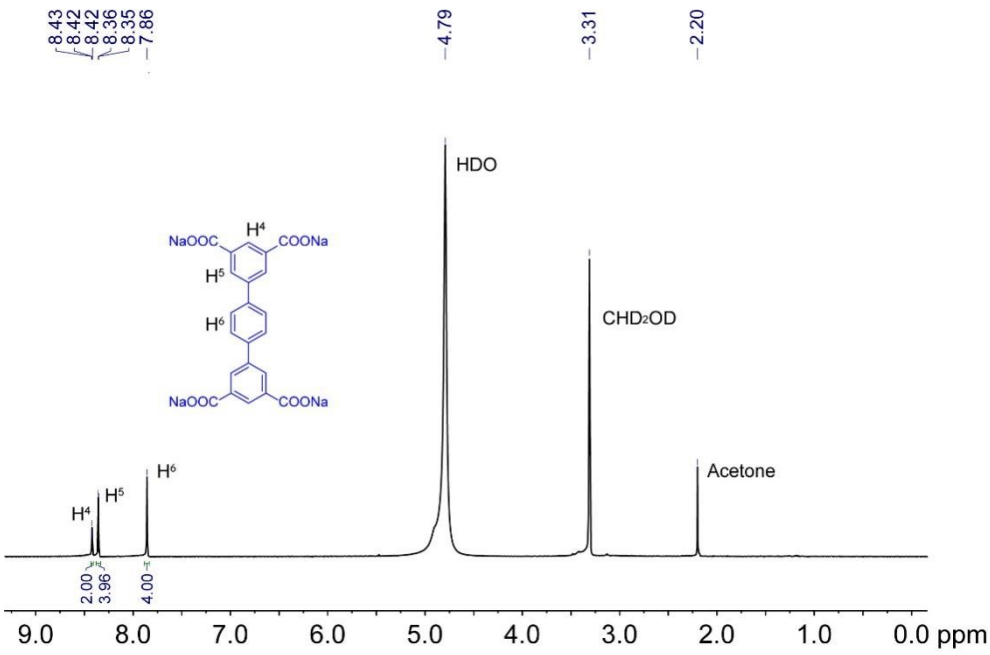

Figure S4. ^{1}H NMR spectrum (600 MHz, CD_3OD, 295 K) recorded for ligand **3c**.

*2.3 Self-assembly of bismetallacycle **4a***

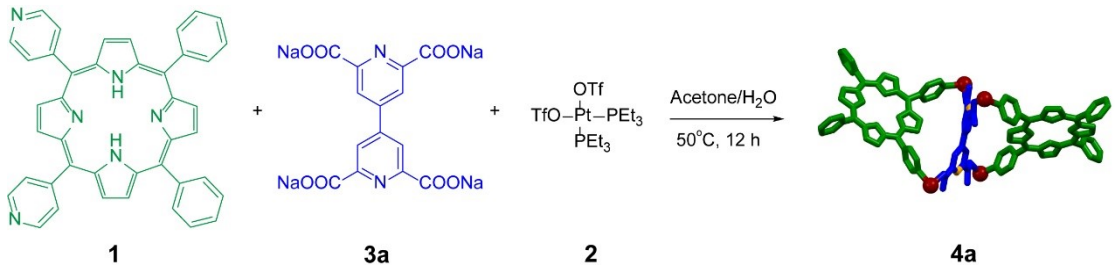

1 (3.00 mg, 4.86 μmol), **3a** (1.02 mg, 2.43 μmol) and **2** (7.10 mg, 9.73 μmol) were mixed in a 2:1:4 molar ratio and dissolved in acetone/water (8 mL, 4:1, v/v). The whole reaction mixture was heated at 50°C for 12 h and then cooled to room temperature. The solvent was removed by nitrogen flow. The residue was redissolved in CH_3CN (1.0 mL) and filtered, and then ethyl ether (4 mL) was added to give a precipitate, which was collected by centrifugation to give bismetallacycle **4a** (8.77 mg, 93%) as a purple red solid. ^{1}H NMR (600 MHz, CD_3CN) δ 9.08 (s, 8H), 8.97 (d, J = 4.7 Hz, 4H), 8.91 (s, 8H), 8.31 (d, J = 5.6 Hz, 8H), 8.21 (d, J = 6.7 Hz, 8H), 8.17 (s, 4H), 7.87 (dd, J = 13.4, 7.3 Hz, 12H), 7.74 (s, 4H), -3.05 (s, 4H). ^{31}P NMR (243 MHz, CD_3CN): 5.85 (d, $^2J_{P\text{-}P}$ = 21.0 Hz, ^{195}Pt satellites, $^1J_{Pt\text{-}P}$ =3361.5 Hz), 1.54 (d, $^2J_{P\text{-}P}$ = 21.0 Hz, ^{195}Pt satellites, $^1J_{Pt\text{-}P}$ =3361.5 Hz). ESI-TOF-MS: m/z 821.7186 [**4a** – 4OTf]$^{4+}$ and m/z 1145.2888 [**4a** – 3OTf]$^{3+}$. TG-DSC: The bismetallacycle **4a** underwent 3.1% of weight loss owing to the removal of trace water and residuary volatile solvents (acetonitrile and isopropyl ether) after heating to 100°C. The 41.7% of weight loss happened between 270 and 500°C was caused by the stabilization of **4a**. Above 500°C, the weight loss tended to be slow with the gradual decomposition of ligands.

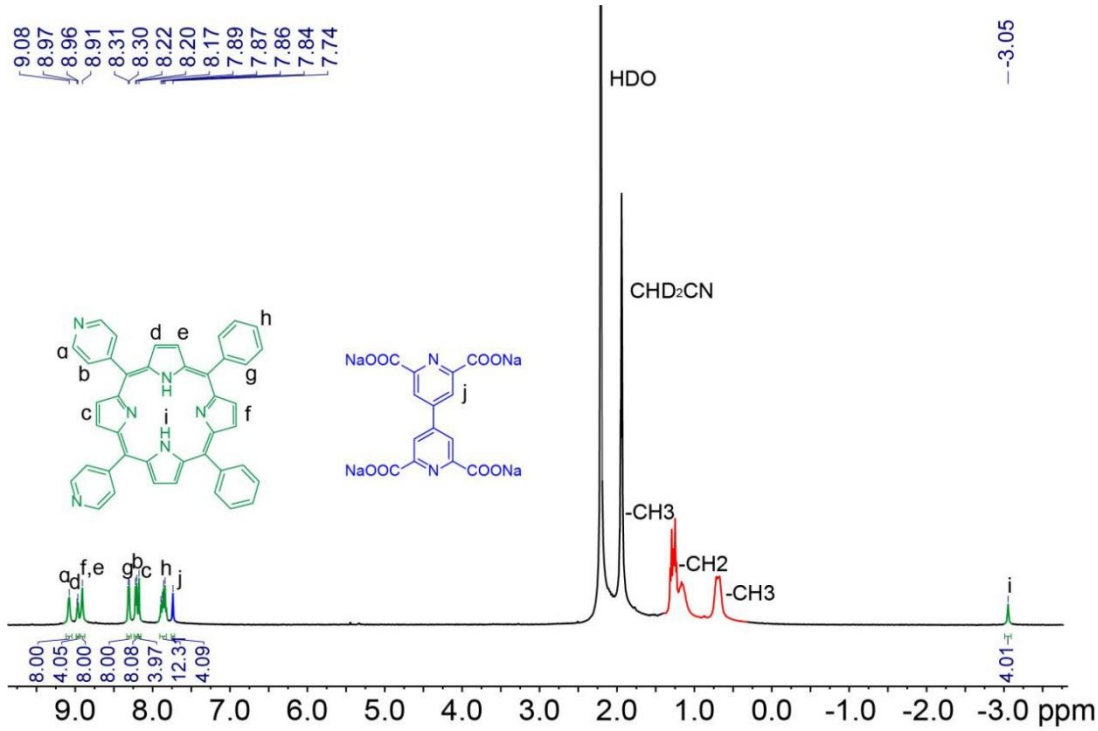

Figure S5. ^{1}H NMR spectrum (600 MHz, CD_3CN, 295 K) recorded for **4a**.

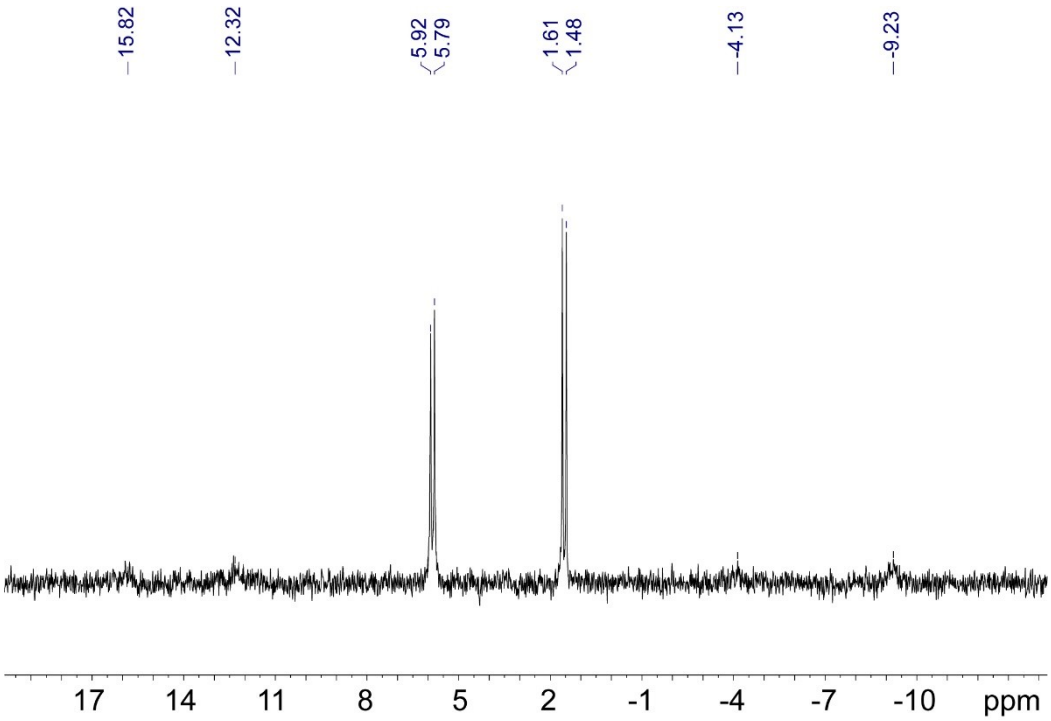

Figure S6. $^{31}P\{^{1}H\}$ NMR spectrum (243 MHz, CD_3CN, 295 K) recorded for **4a**.

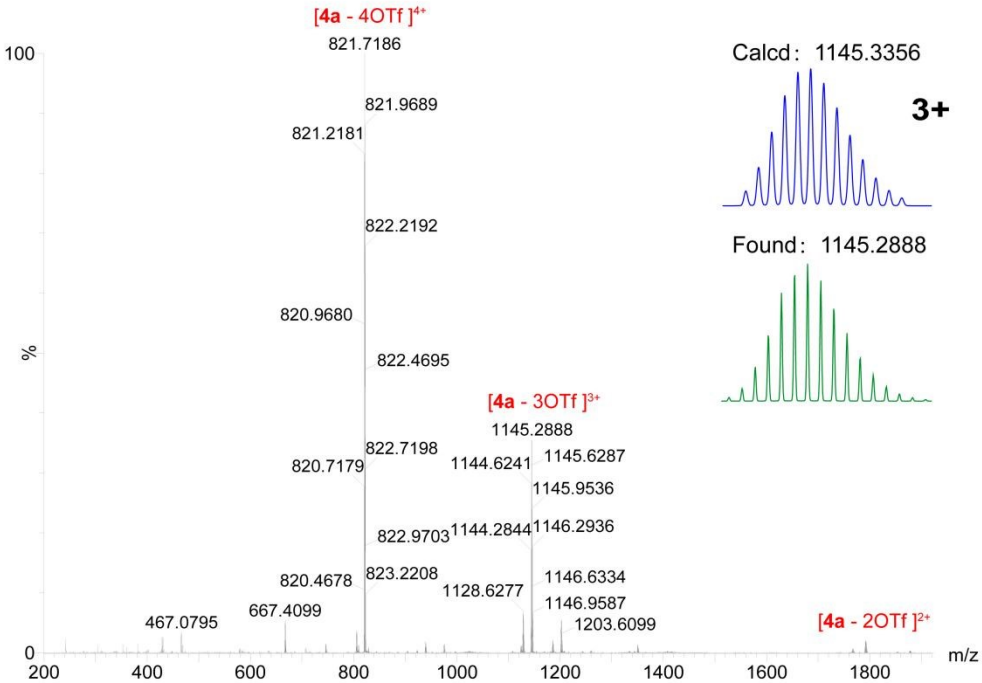

Figure S7. ESI-TOF-MS spectrum of **4a**.

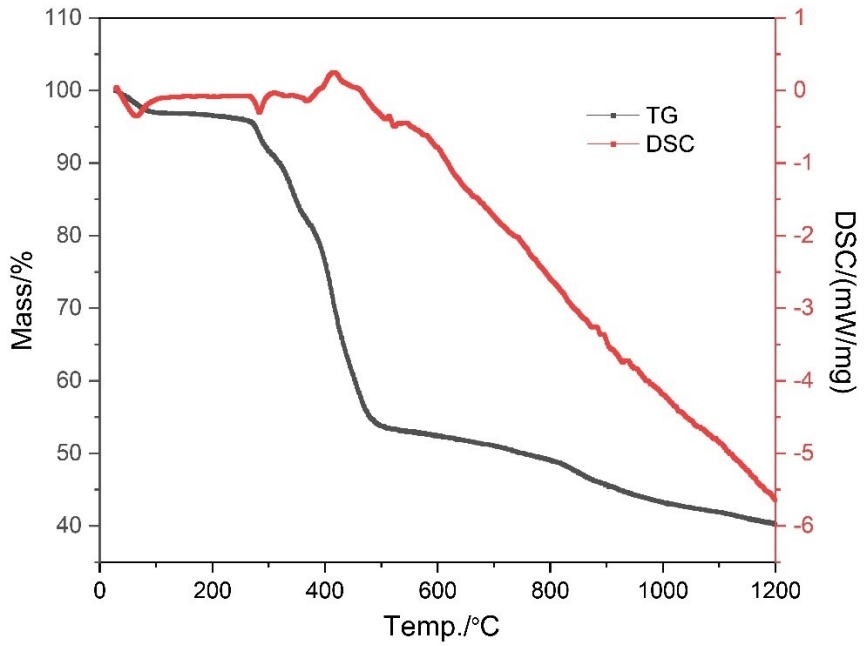

Figure S8. TG-DSC curve of **4a**.

*2.4 Self-assembly of bismetallacycle **4b***

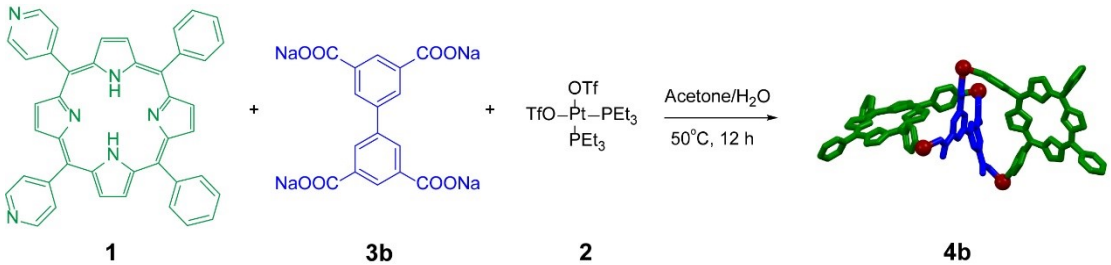

1 (3.00 mg, 4.86 μmol), **3b** (1.02 mg, 2.43 μmol) and **2** (7.10 mg, 9.73 μmol) were mixed in a 2:1:4 molar ratio and dissolved in acetone/water (8 mL, 4:1, v/v). The whole reaction mixture was heated at 50°C for 12 h and then cooled to room temperature. The solvent was removed by nitrogen flow. The residue was redissolved in CH_3CN (1.0 mL) and filtered, and then ethyl ether (4 mL) was added to give a precipitate, which was collected by centrifugation to give bismetallacycle **4b** (9.05 mg, 96%) as a purple red solid. ^{1}H NMR (600 MHz, CD_3CN) δ 9.08 (s, 8H), 8.94 (s, 4H), 8.90 (s, 4H), 8.85 (s, 4H), 8.37 (s, 4H), 8.29 (s, 8H), 8.20 (d, J = 6.8 Hz, 8H), 8.07 (s, 2H), 7.86 (dd, J = 22.0, 6.7 Hz, 12H), 7.71 (s, 4H), -3.06 (s, 4H). ^{31}P NMR (243 MHz, CD_3CN): 5.56 (d, $^2J_{P\text{-}P}$ = 21.0 Hz, ^{195}Pt satellites, $^1J_{Pt\text{-}P}$ =3376.5 Hz), 1.17(d, $^2J_{P\text{-}P}$ = 21.0 Hz, ^{195}Pt satellites, $^1J_{Pt\text{-}P}$ =3376.5 Hz). ESI-TOF-MS: m/z 821.2181 [**4b** – 4OTf]$^{4+}$ and m/z 1144.6241 [**4b** – 3OTf]$^{3+}$. TG-DSC: The bismetallacycle **4b** underwent 3.3% of weight loss owing to the removal of trace water and residuary volatile solvents (acetonitrile and isopropyl ether) after heating to 100°C. The 41.9% of weight loss happened between 270 and 500°C was caused by the stabilization of **4b**. Above 500°C, the weight loss tended to be slow with the gradual decomposition of ligands.

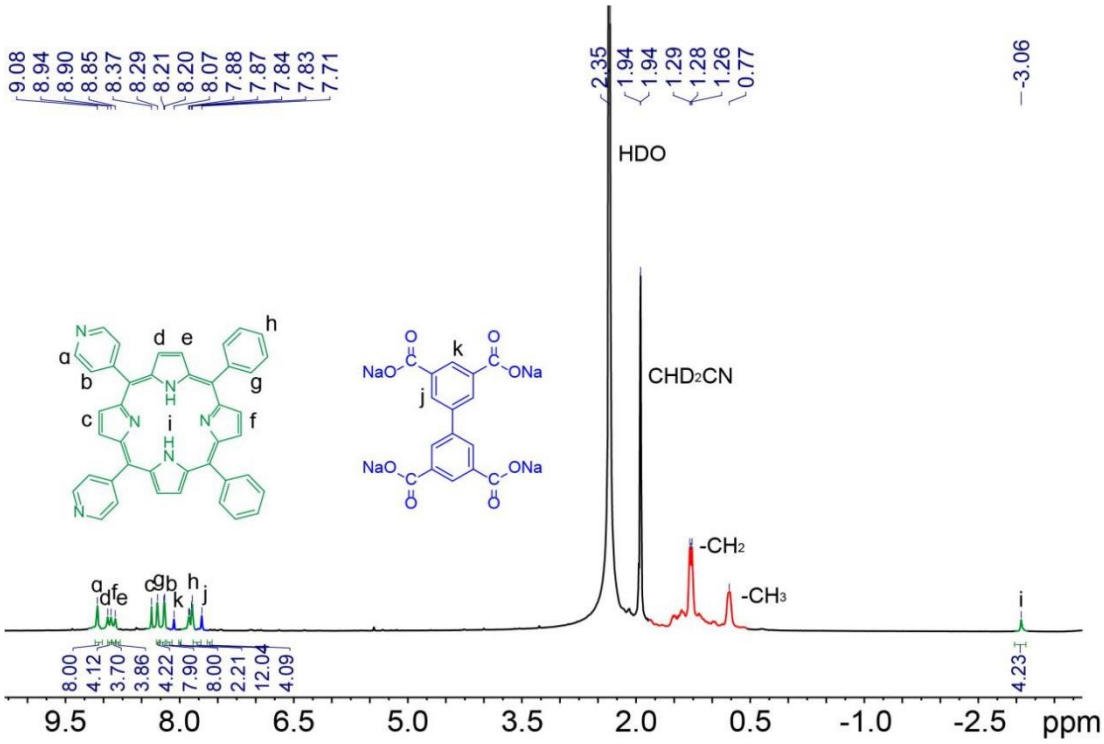

Figure S9. ^{1}H NMR spectrum (600 MHz, CD_3CN, 295 K) recorded for **4b**.

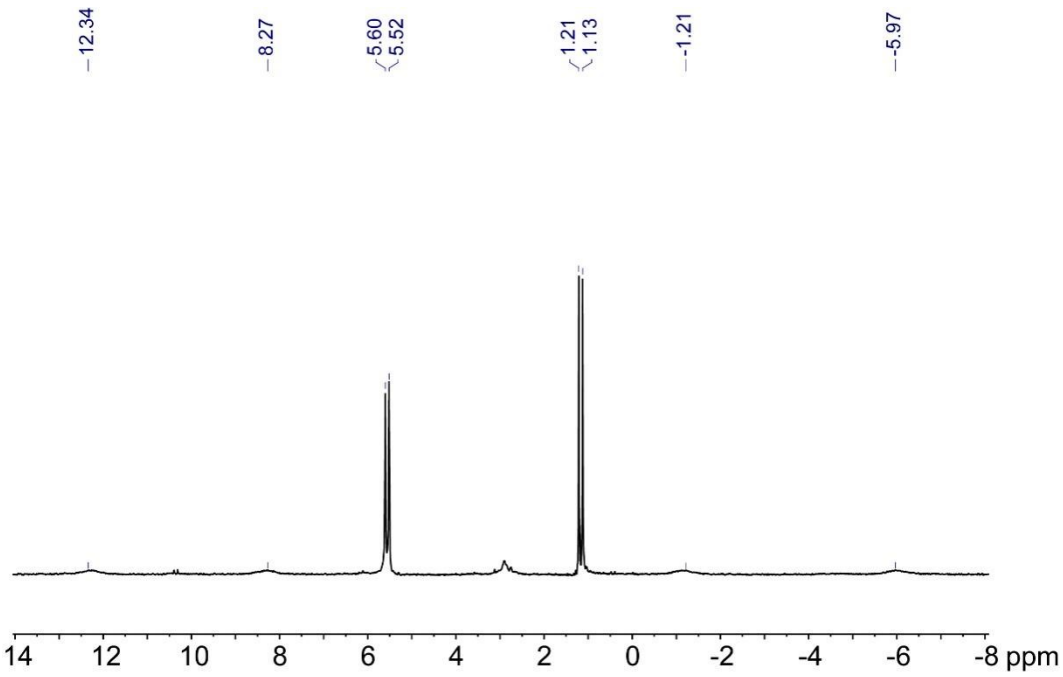

Figure S10. ^{31}P{^{1}H} NMR spectrum (243 MHz, CD_3CN, 295 K) recorded for **4b**.

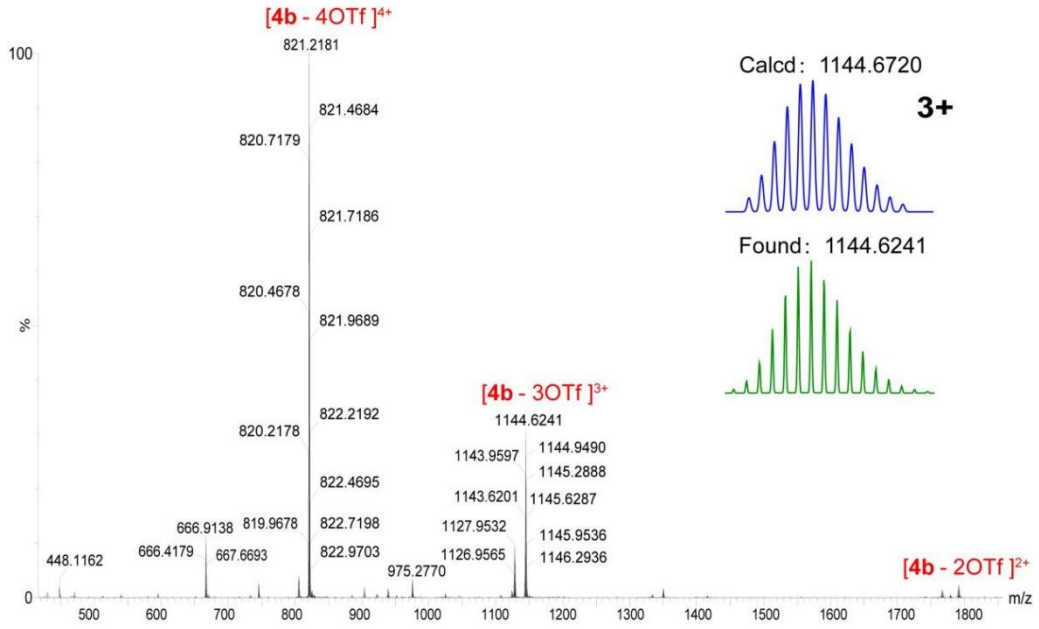

Figure S11. ESI-TOF-MS spectrum of **4b**.

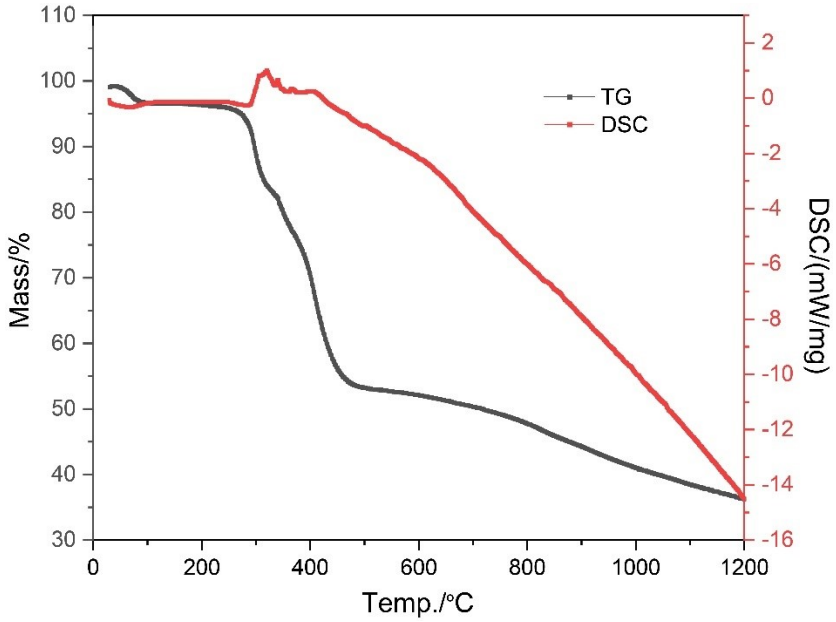

Figure S12. TG-DSC curve of **4b**.

*2.5 Self-assembly of bismetallacycle **4c***

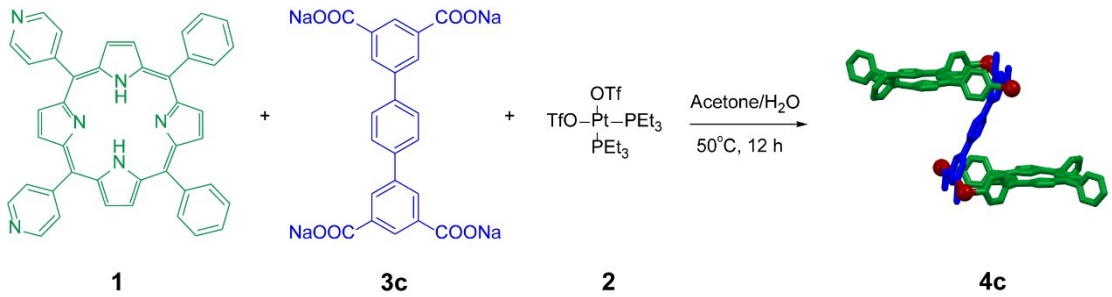

1 (3.00 mg, 4.86 μmol), **3c** (1.20 mg, 2.43 μmol) and **2** (7.10 mg, 9.73 μmol) were mixed in a 2:1:4 molar ratio and dissolved in acetone/water (8 mL, 4:1, v/v). The whole reaction mixture was heated at 50°C for 12 h and then cooled to room temperature. The solvent was removed by nitrogen flow. The residue was redissolved in CH_3CN (1.0 mL) and filtered, and then ethyl ether (4 mL) was added to give a precipitate, which was collected by centrifugation to give bismetallacycle **4c** (7.88 mg, 82%) as a purple red solid. ^{1}H NMR (600 MHz, CD_3CN) δ 9.08 (s, 4H), 9.04 (s, 8H), 8.98 (s, 4H), 8.81 (s, 7H), 8.62 (s, 2H), 8.22 (d, J = 1.3 Hz, 4H), 8.18 (d, J = 5.1 Hz, 7H), 8.16 (d, J = 7.0 Hz, 8H), 7.83 (dt, J = 37.0, 7.5 Hz, 12H), 7.51 (s, 4H), -3.16 (s, 4H). ^{31}P NMR (243 MHz, CD_3CN): δ 6.71 (d, $^2J_{P\text{-}P}$ = 21.4 Hz, ^{195}Pt satellites, $^1J_{Pt\text{-}P}$ =3320.6 Hz), 0.97 (d, $^2J_{P\text{-}P}$ = 21.4 Hz, ^{195}Pt satellites, $^1J_{Pt\text{-}P}$ =3320.6 Hz). ESI-TOF-MS: m/z 840.2023 [**4c** – 4OTf]$^{4+}$, m/z 1169.5986 [**4c** – 3OTf]$^{3+}$ and m/z 1829.3933 [**4c** – 2OTf]$^{2+}$. TG-DSC: The bismetallacycle **4c** underwent 3.8% of weight loss owing to the removal of trace water and residuary volatile solvents (acetonitrile and isopropyl ether) after heating to 100°C. The 42.5% of weight loss happened between 270 and 500°C was caused by the stabilization of **4c**. Above 500°C, the weight loss tended to be slow with the gradual decomposition of ligands.

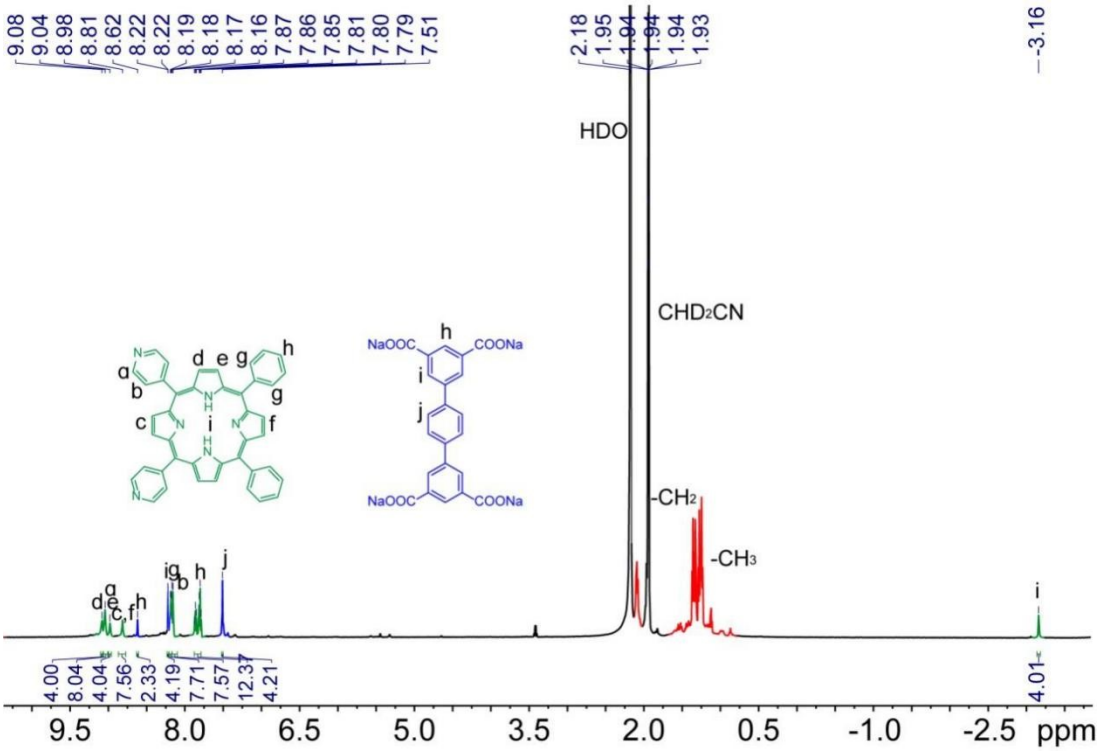

Figure S13. ^{1}H NMR spectrum (600 MHz, CD_3CN, 295 K) recorded for **4c**.

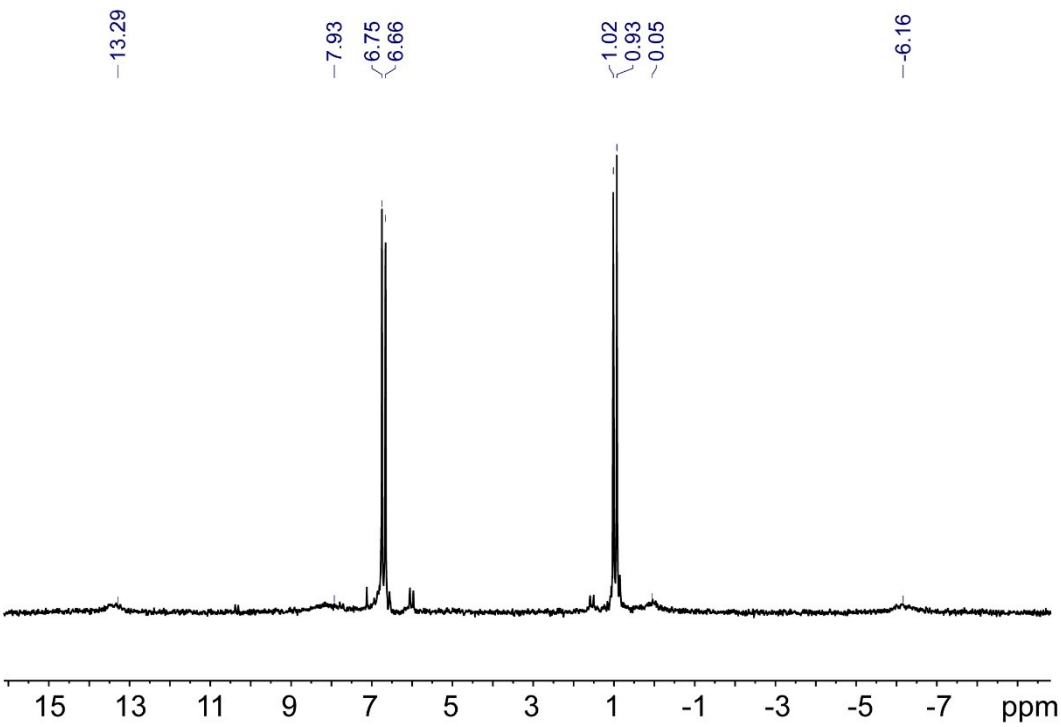

Figure S14. ^{1}H NMR spectrum (243 MHz, CD_3CN, 295 K) recorded for **4c**.

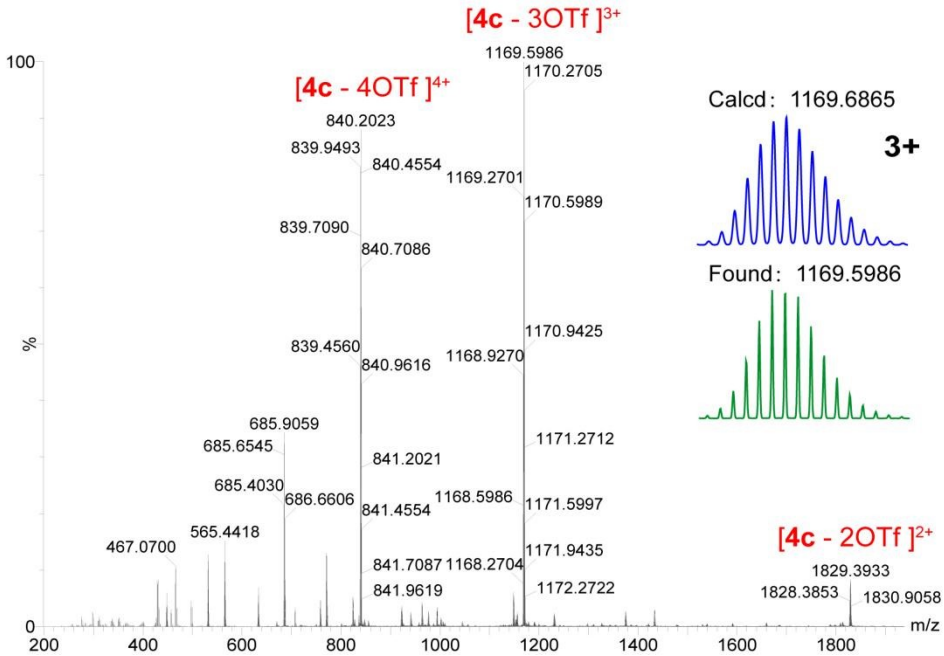

Figure S15. ESI-TOF-MS spectrum of **4c**.

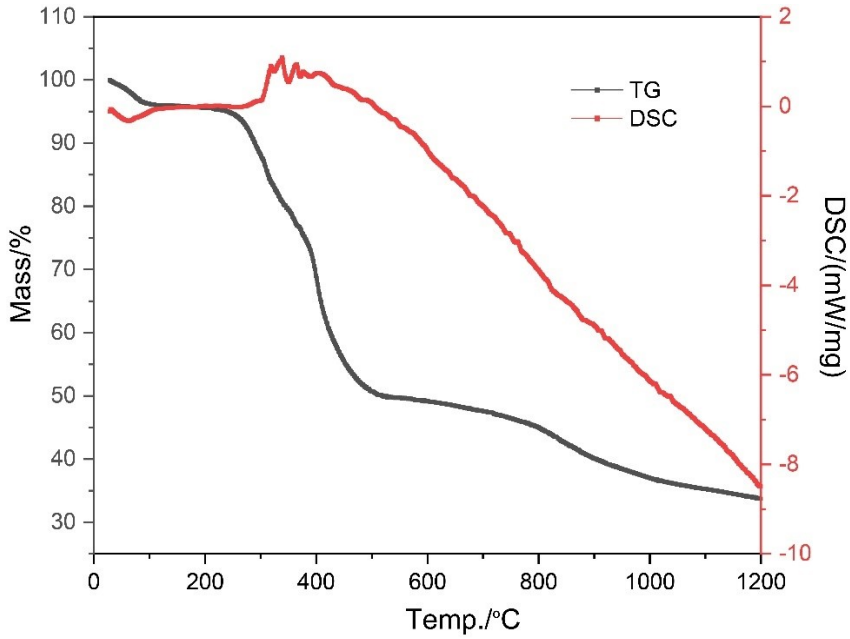

Figure S16. TG-DSC curve of **4c**.

3. Crystallographic data and refinement details

The structures were tested using a high brightness MetalJet Ga X-ray light source. When tested at low temperature of 193K, the diffractions of these samples were still very weak. Although we have tried many crystals, there is still not much change. Considering that these structures have huge unit cells, this is a normal phenomenon.

In the refinement of the bismetallacycles, the contents of solvent mask have been investigated by the TG-DSC and mass spectrum results, combined with the number of masked electrons. Furthermore, these moieties were presented in the moiety formula and were parts of the sum formula. For bismetallacycle **4a**, the solvent mask was used to calculate the number of solvent molecules, including fifteen acetonitrile and six isopropyl ether molecules. In order to make the structure chemically reasonable, DFIX, SADI, FLAT, RIGU, SAME and other instructions were used to limit the geometry of the structure, while using ISOR and SIMU to limit the temperature factor of atoms. Pt4 and Pt4a were subjected to disorderly refinement, with the heaviest ratio of 0.3438/0.6562. Due to the large unit cells and weak diffraction, there are more disordered solvents in the structure, which cannot be refined to obtain a reasonable structure. Therefore, the SQUEEZE function of PLATON is used to remove them, and the number of electrons removed is 9802. Finally, the crystal data we obtained is R1 = 15.71%. For bismetallacycle **4b**, the solvent mask was used to calculate the number of solvent molecules, including sixteen acetonitrile and five isopropyl ether molecules to be part of the sum formula. And the restraints command of DFIX, SADI, SIMU, DELU, ISOR was used to make the structure chemically reasonable. The number and ratio of four Pt atoms are 0.95/0.05. And residual electron density of **4b** is 9.20. The crystal data we finally obtained is R1 = 11.57 %. For bismetallacycle **4c**, the solvent mask was

used to calculate the number of solvent molecules combined with the TG-DSC data, MS results and the number of masked electrons, including thirteen acetonitrile and five isopropyl ether molecules to be part of the sum formula. And the restraints command of DFIX, SADI, SIMU, DELU, ISOR was used to make the structure chemically reasonable. The crystal data we finally obtained is R1 = 9.73 %, all of which are the best results we obtained.

Table S1. Crystallographic data and refinement details for bismetallacycle **4a**.

Compound	**4a**
Sum formula	$C_{212}H_{305}N_{29}O_{14}P_8Pt_4$
Space group	C 2/c
Hall group	-C 2yc
Mr	4511.95
a /Å	60.979(7)
b /Å	64.130(7)
c /Å	23.452(3)
α /°	90
β /°	95.388(6)
γ /°	90
V /Å^3	91305(18)
Z	16
Dx, g cm^{-3}	1.312
F (000)	26336
μ /mm^{-1}	3.624
h,k,l max	70,74,27
θ max	51.441
Reflns [I >2σ(I)]	75534
R_1; ωR_2 [I >2σ(I)]	0.1571; 0.4072
GOOF	1.159

Table S2. Crystallographic data and refinement details for bismetallacycle **4b**.

Compound	**4b**
Sum formula	$C_{210}H_{296}N_{28}O_{13}P_8Pt_4$
Space group	C 1 2/c 1
Hall group	-C 2yc
Mr	4448.85
a /Å	31.577(4)
b /Å	32.060(4)
c /Å	39.781(4)
α /°	90
β /°	93.216(7)

γ /°	90
V /Å^3	40210(7)
Z	8
Dx, g cm^{-3}	1.470
F (000)	18304
μ /mm^{-1}	2.881
h,k,l max	37,37,46
θ max	24.713
Reflns [I >2σ(I)]	34193
R_1; ωR_2 [I >2σ(I)]	0.1157; 0.0920
GOOF	1.188

Table S3. Crystallographic data and refinement details for bismetallacycle **4c**.

Compound	**4c**
Sum formula	$C_{210}H_{291}N_{25}O_{13}P_8Pt_4$
Space group	C 1 2/c 1
Hall group	-C 2yc
Mr	4401.78
a /Å	53.469(13)
b /Å	26.692(6)
c /Å	37.842(10)
α /°	90
β /°	134.806(19)
γ /°	90
V /Å^3	38319(18)
Z	8
Dx, g cm^{-3}	1.526
F (000)	18096
μ /mm^{-1}	3.024
h,k,l max	63,31,44
θ max	24.901
Reflns [I >2σ(I)]	33330
R_1; ωR_2 [I >2σ(I)]	0.0973; 0.0869
GOOF	1.084

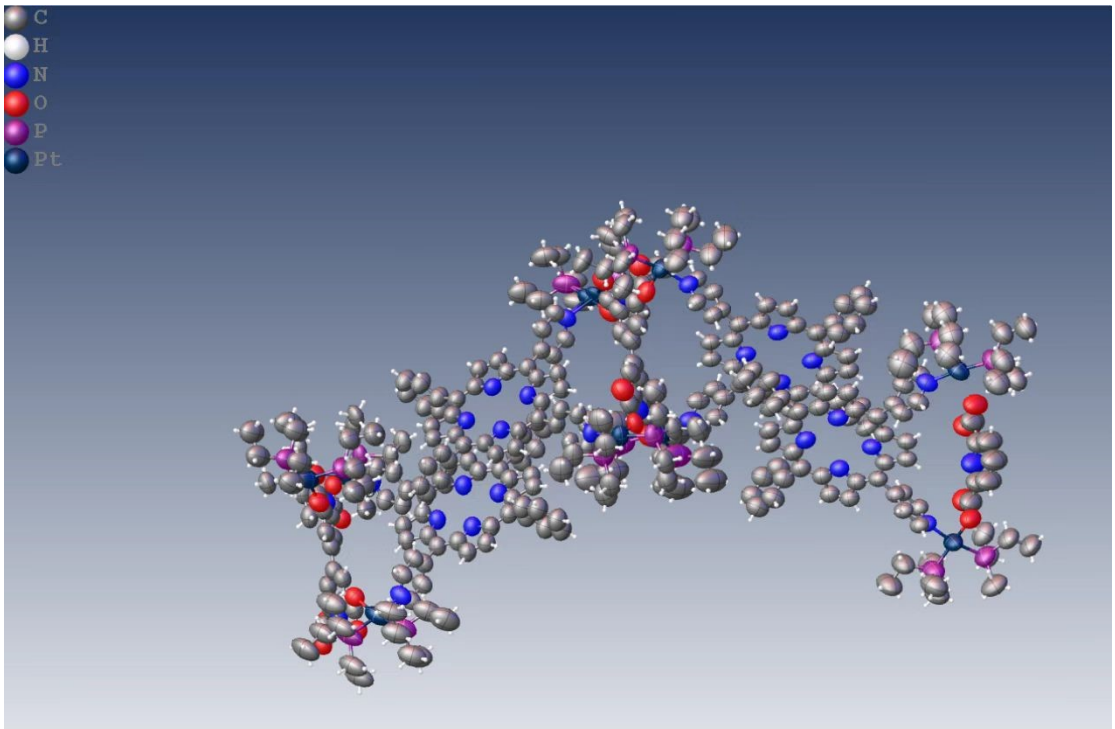

Figure S17. Ellipsoid plot of the bismetallacycle **4a**.

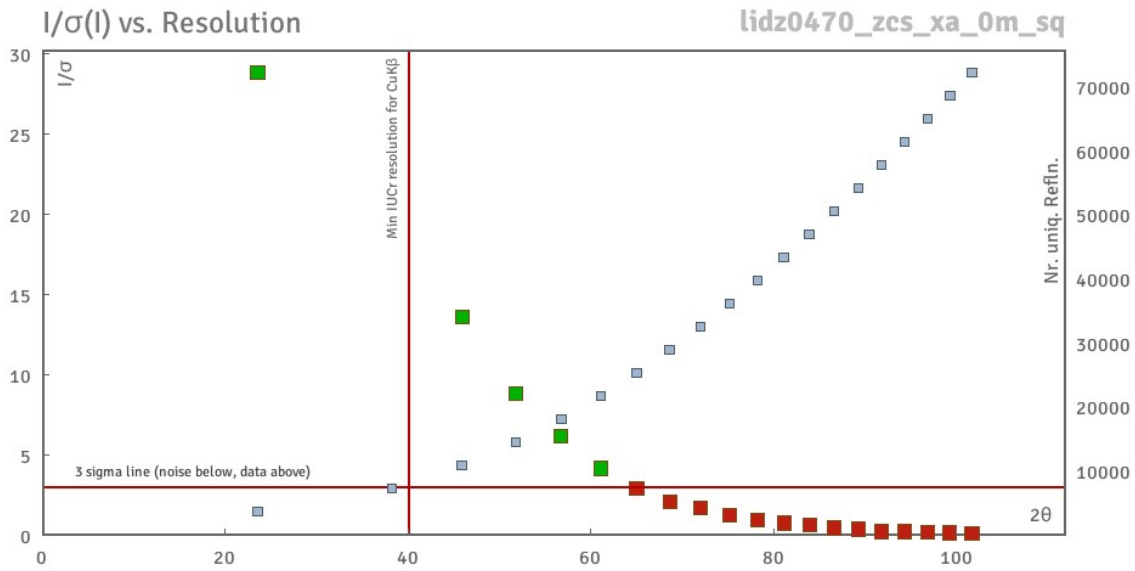

Figure S18. I/σ(I) vs. Resolution plot of the bismetallacycle **4a**.

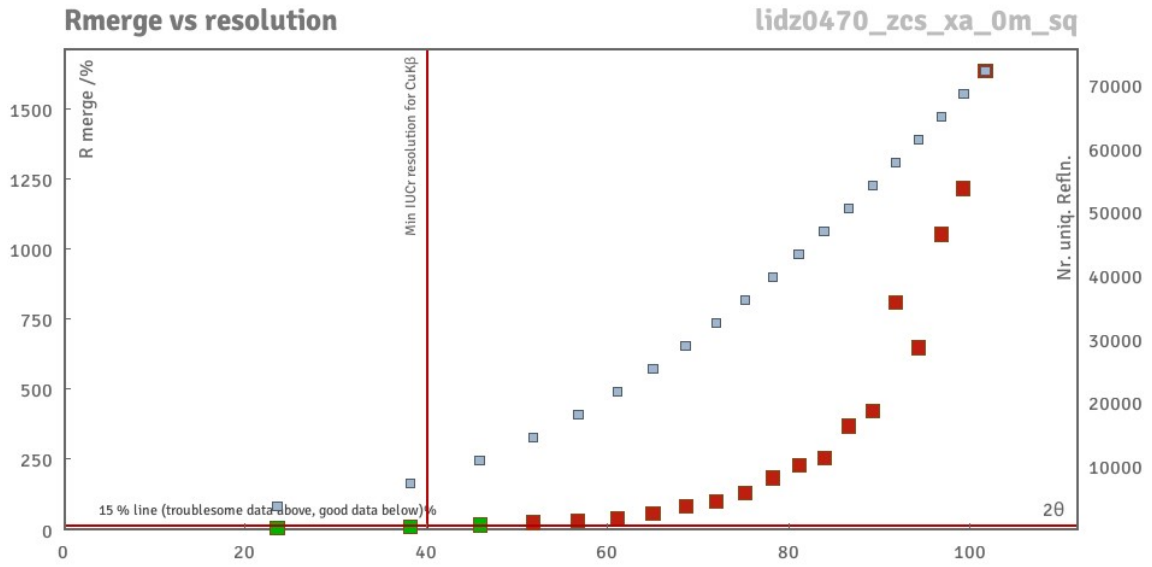

Figure S19. Remerge vs resolution plot of the bismetallacycle **4a**.

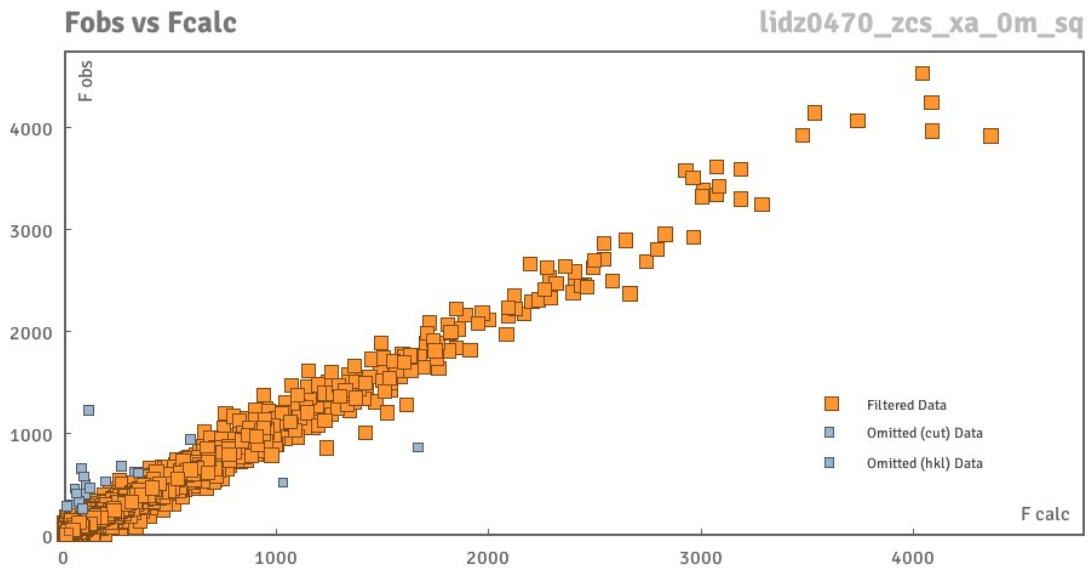

Figure S20. Fobs vs Fcalc plot of the bismetallacycle **4a**.

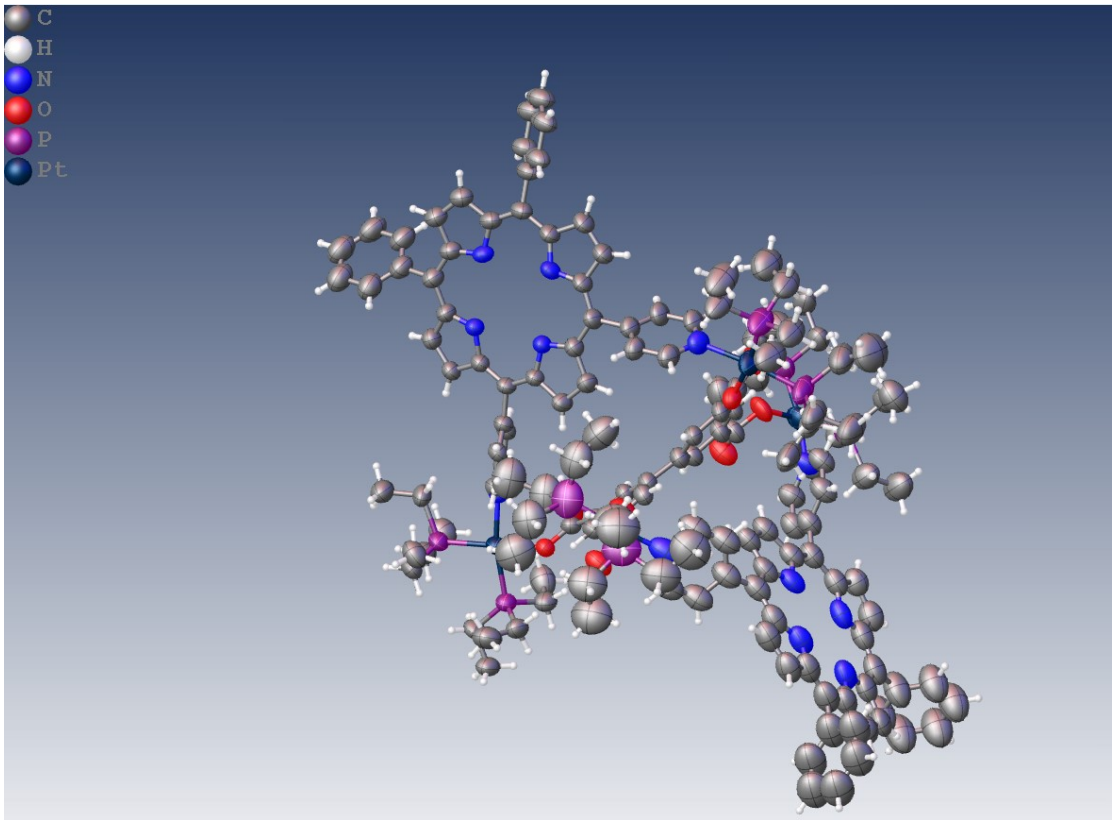

Figure S21. Ellipsoid plot of the bismetallacycle **4b**.

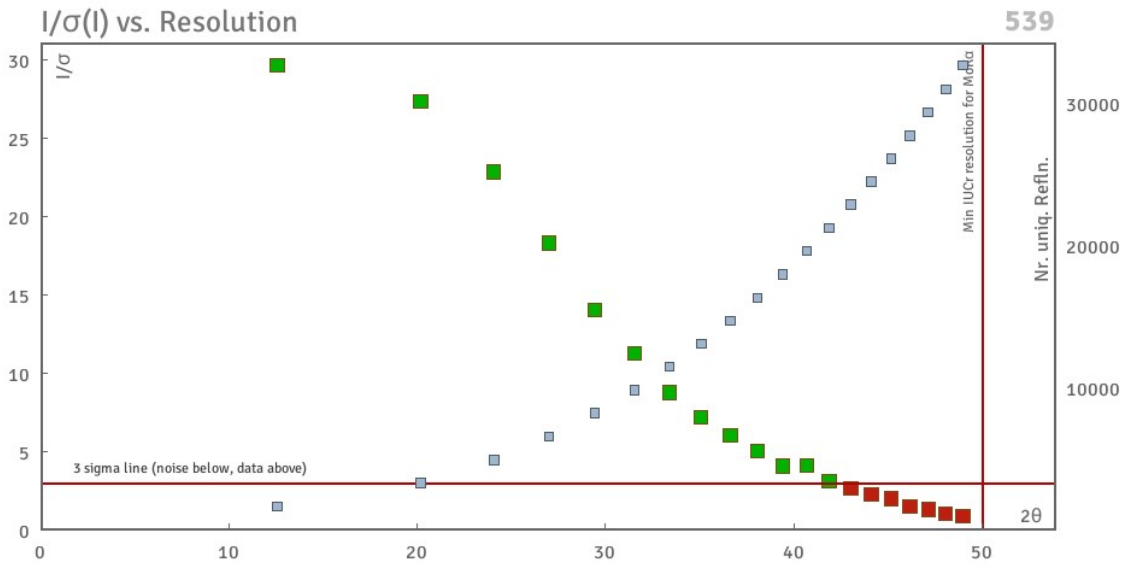

Figure S22. I/σ(I) vs. Resolution plot of the bismetallacycle **4b**.

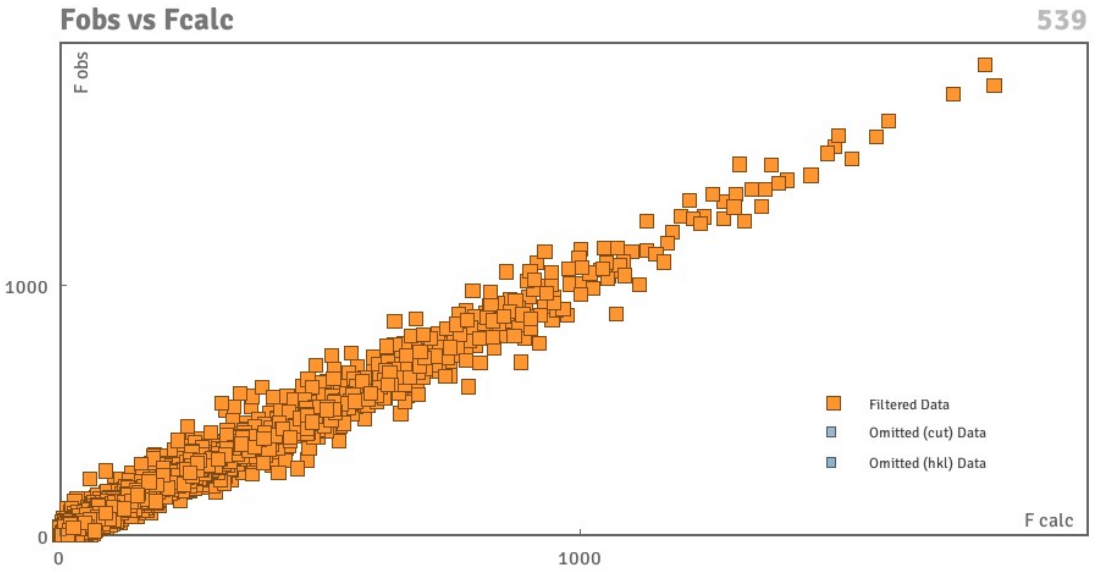

Figure S23. Fobs vs Fcalc plot of the bismetallacycle **4b**.

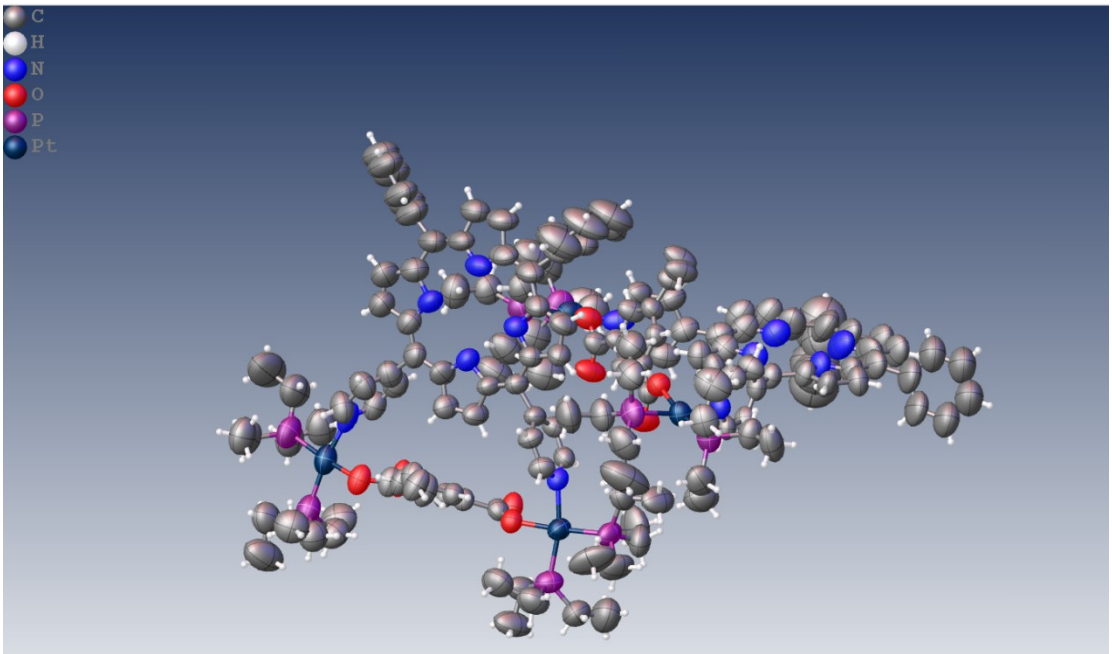

Figure S24. Ellipsoid plot of the bismetallacycle **4c**.

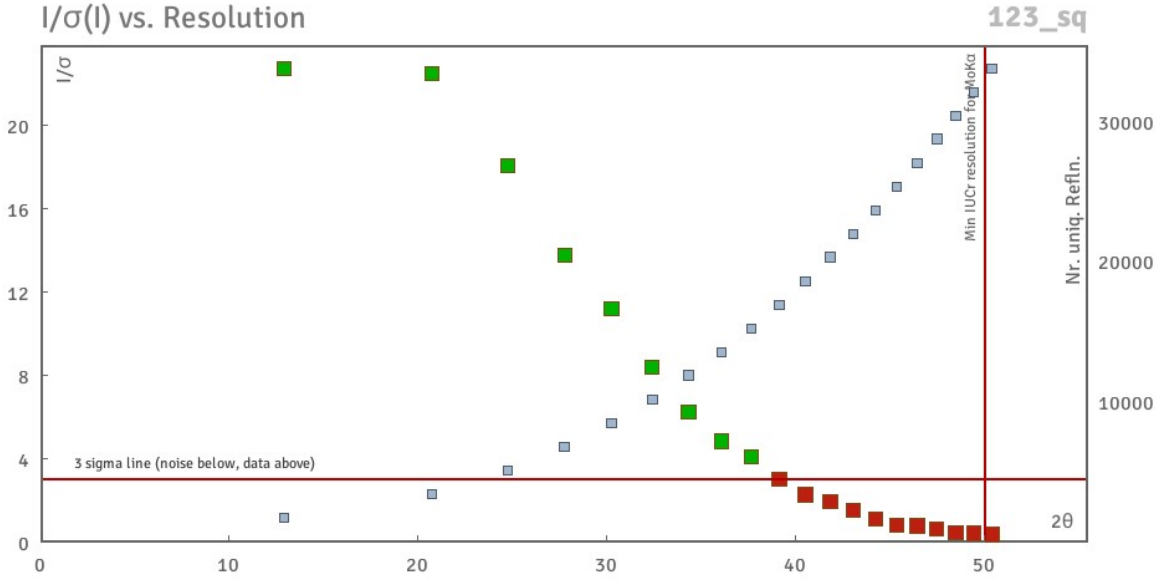

Figure S25. I/σ(I) vs. Resolution plot of the bismetallacycle **4c**.

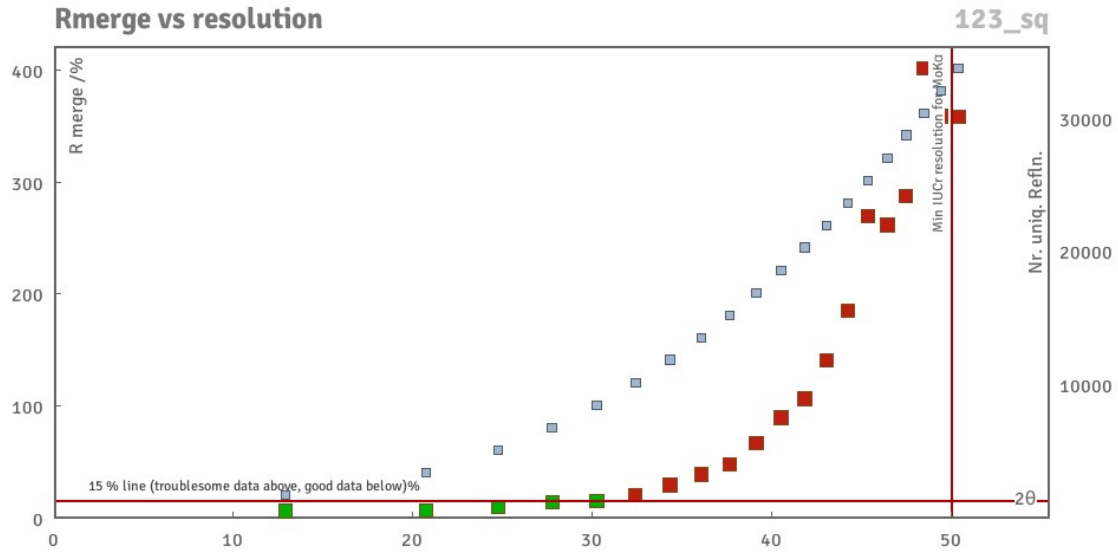

Figure S26. Remerge vs resolution plot of the bismetallacycle **4c**.

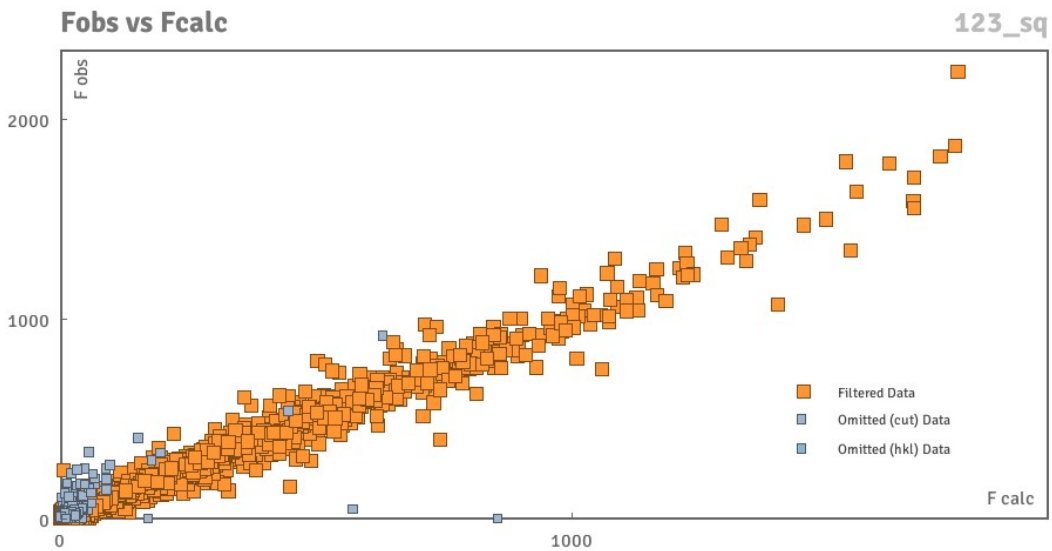

Figure S27. Fobs vs Fcalc plot of the bismetallacycle **4c**.

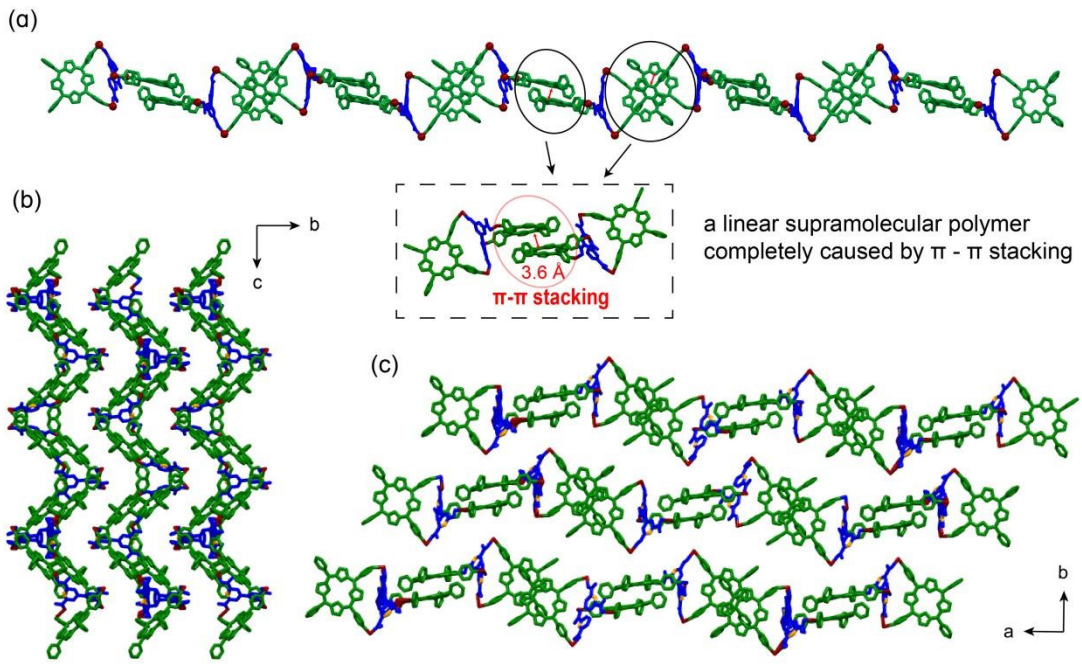

Figure S28. Crystal packing model of bismetallacycle **4a**. Hydrogen atoms, counterions, triethylphosphine units and solvent molecules are omitted for clarity.

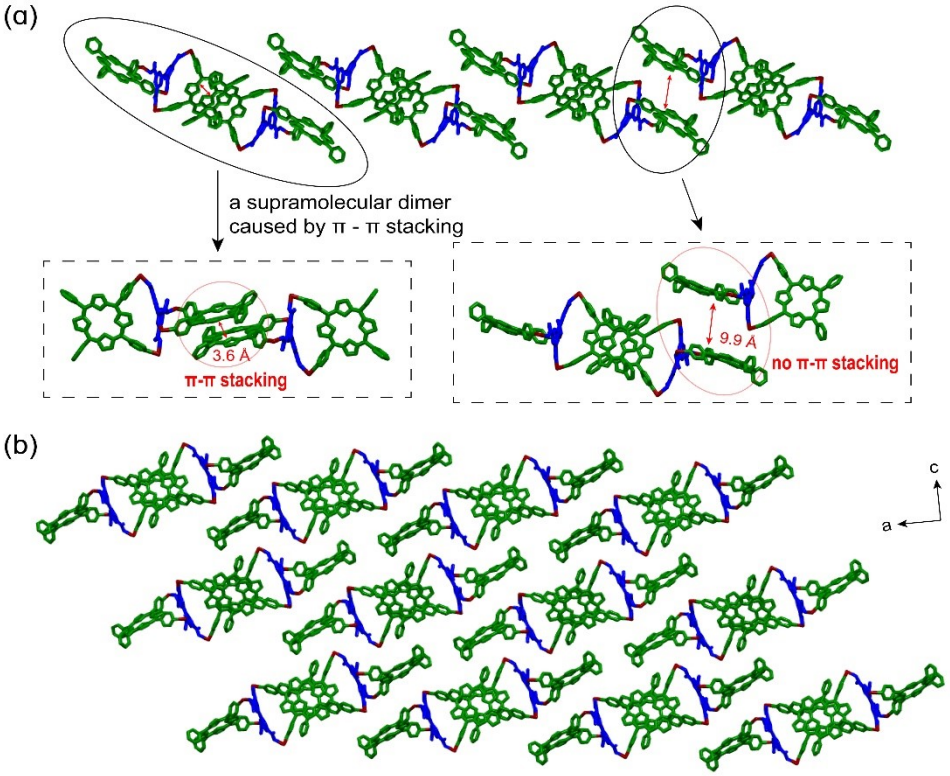

Figure S29. Crystal packing model of bismetallacycle **4b**. Hydrogen atoms, counterions, triethylphosphine units and solvent molecules are omitted for clarity.

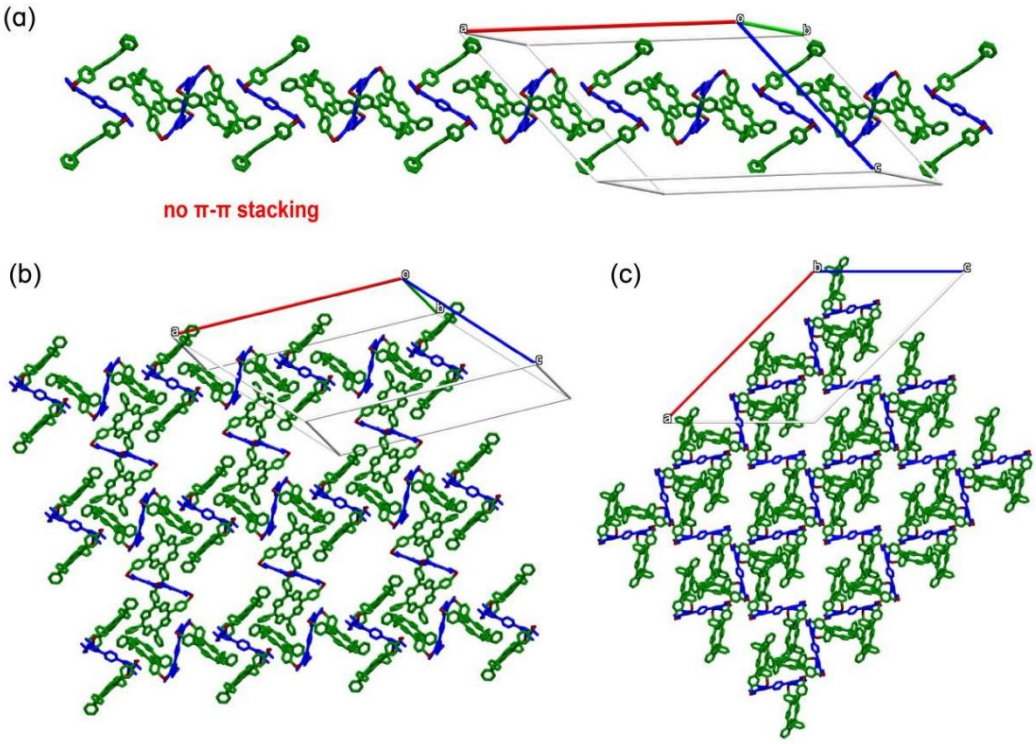

Figure S30. Crystal packing model of bismetallacycle **4c**. Hydrogen atoms, counterions, triethylphosphine units and solvent molecules are omitted for clarity.

4. Measurements of absolute fluorescence quantum yields

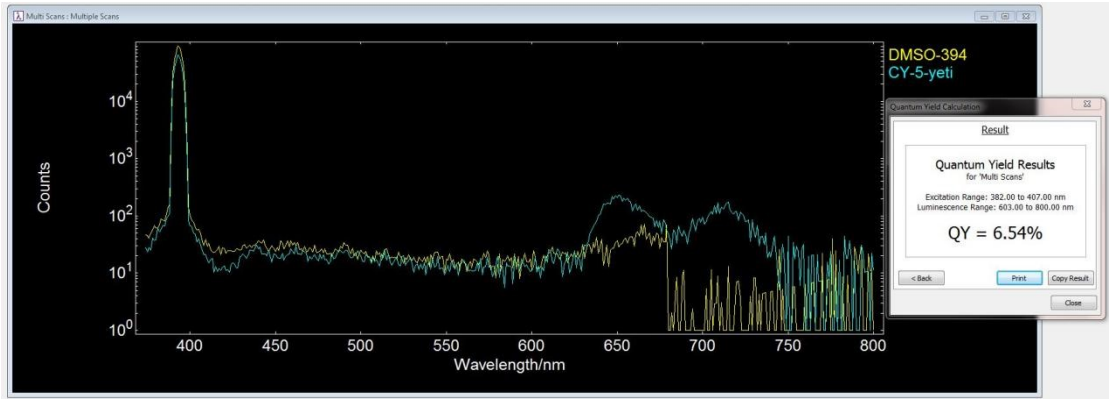

Figure S31. Absolute fluorescence quantum yield of ligand **1** in DMSO.

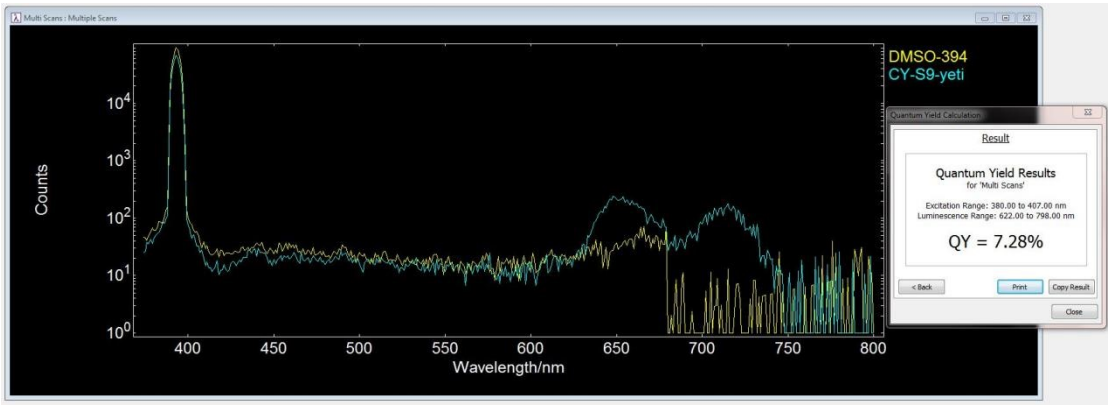

Figure S32. Absolute fluorescence quantum yield of bismetallacycle **4a** in DMSO

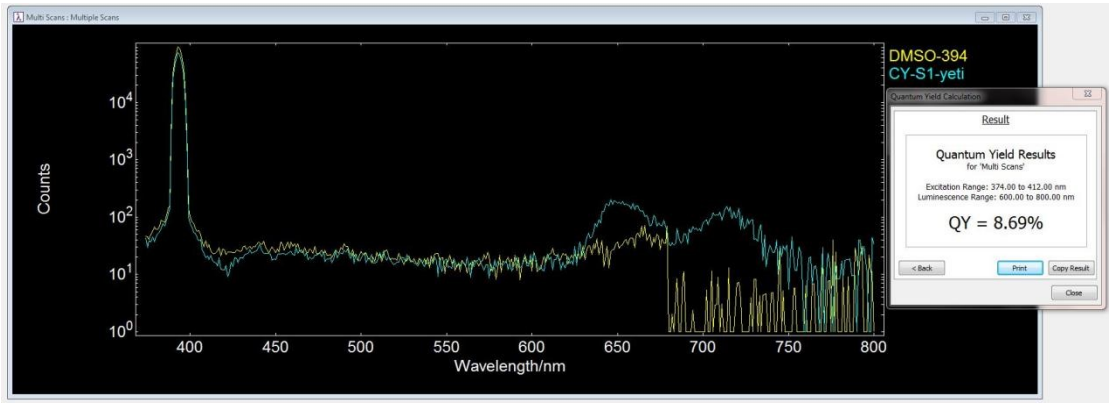

Figure S33. Absolute fluorescence quantum yield of bismetallacycle **4b** in DMSO.

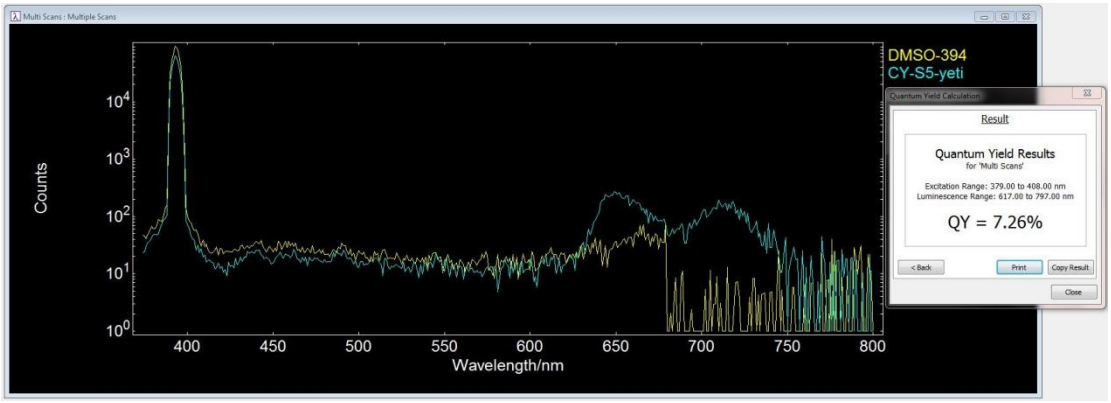

Figure S34. Absolute fluorescence quantum yield of bismetallacycle **4c** in DMSO.

5. UV–vis absorption and emission spectra in different solvents

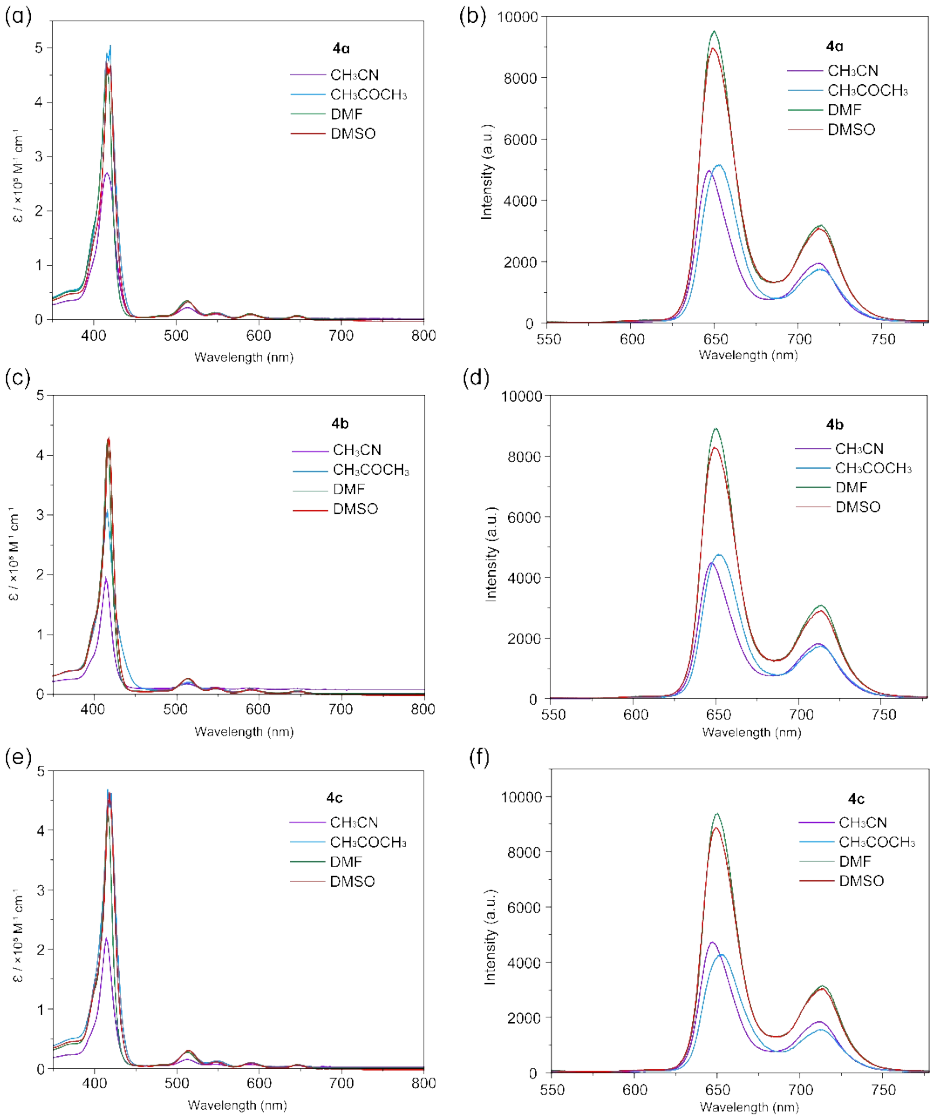

Figure S35. The UV/Vis absorption (a, c, e) and emission (b, d, f) spectra of bismetallacycles **4a** (a, b), **4b** (c, d) and **4c** (e, f) in different solvents (λ_{ex} = 394 nm, c = 10.0 μM).

6. Singlet oxygen test of control sample

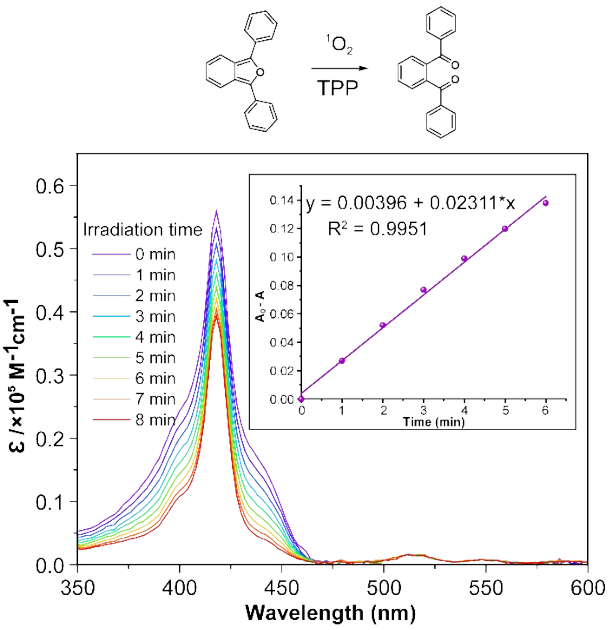

Figure S36. Time dependent UV/vis absorption of the mixture of DPBF with TPP. Inset： The plot for the absorption decays of DPBF at 418 nm upon light irradiation in the presence of TPP (λ_{ex} = 405 nm, DMSO).

7. Photocatalytic oxidation study of different porphyrin photosensitizers

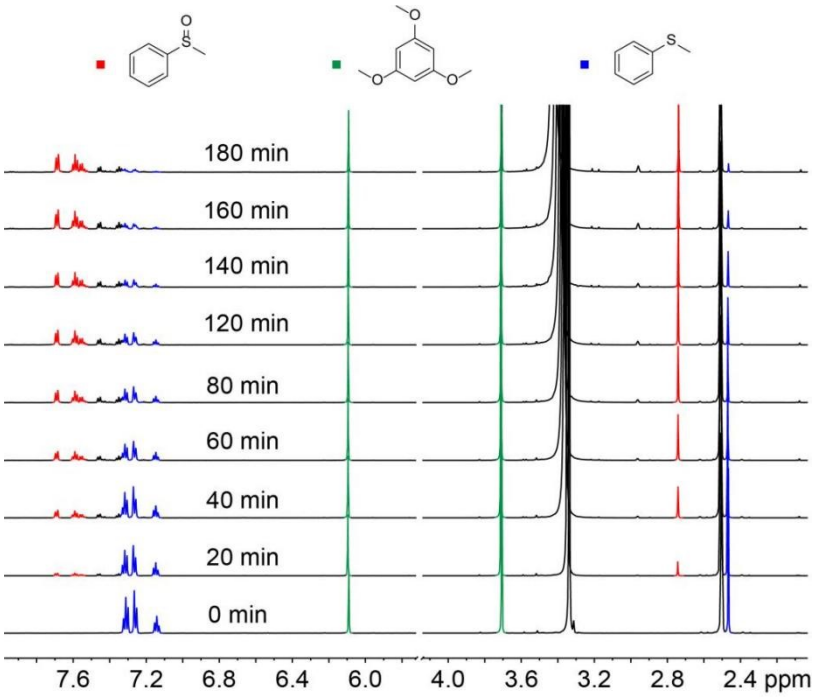

Figure S37. Time-dependent ^{1}H NMR spectra (600 MHz, DMSO, 295 K) of the oxidation of MPS using 1 mol% ligand **1** as the photosensitizer

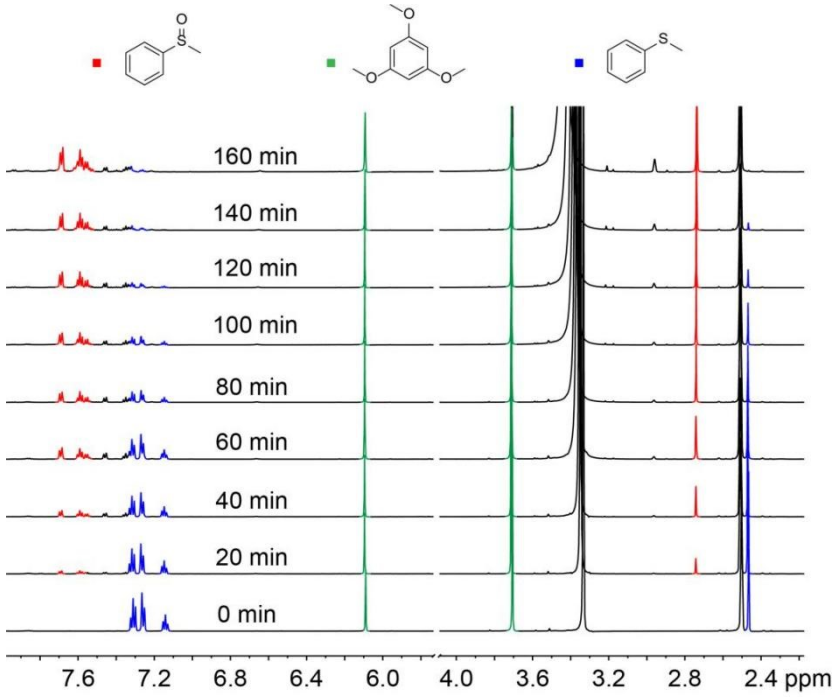

Figure S38. Time-dependent ^{1}H NMR spectra (600 MHz, DMSO, 295 K) of the oxidation of MPS using 1 mol% **4a** as the photosensitizer

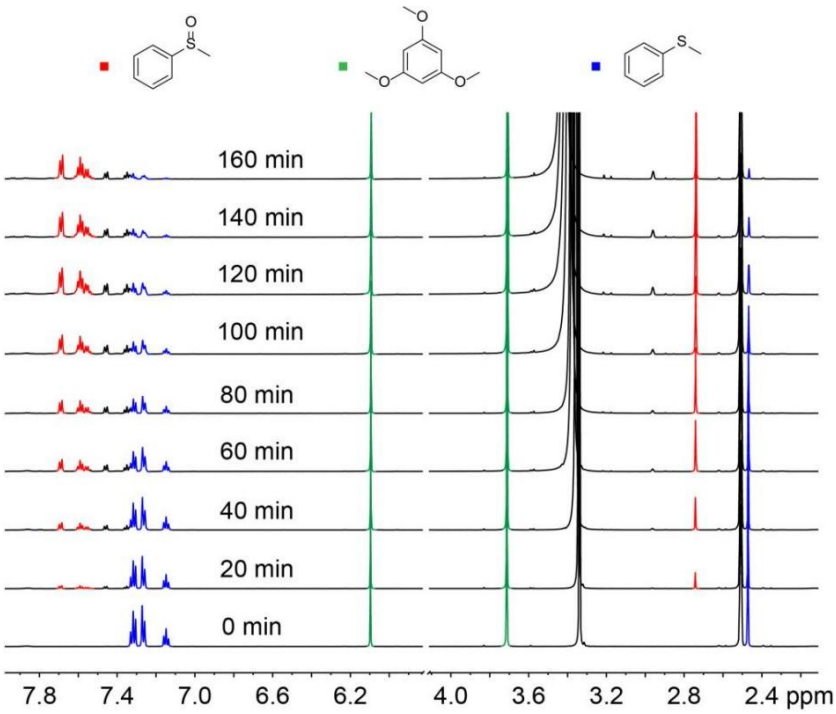

Figure S39. Time-dependent ^{1}H NMR spectra (600 MHz, DMSO, 295 K) of the oxidation of MPS using 1 mol% **4b** as the photosensitizer

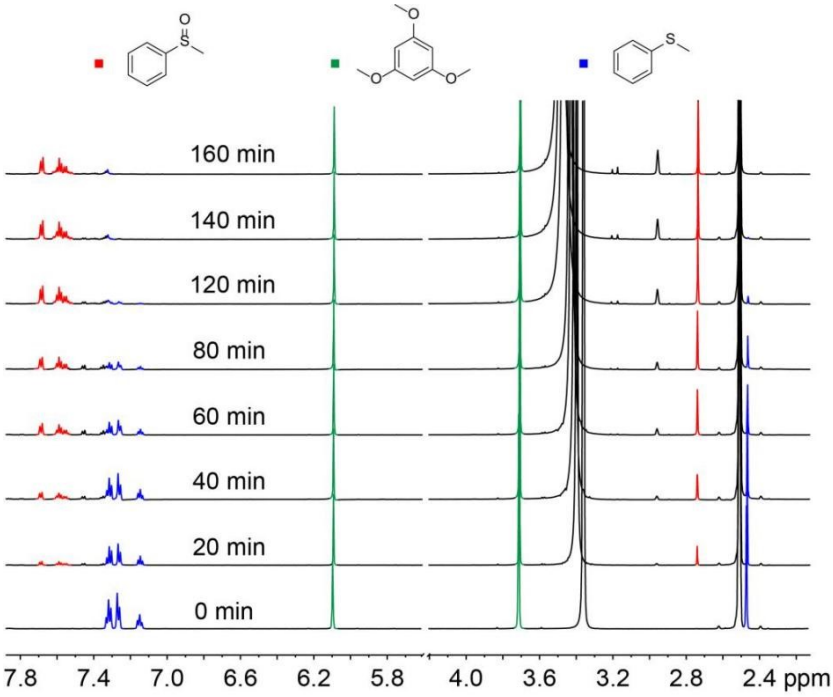

Figure S40. Time-dependent ^{1}H NMR spectra (600 MHz, DMSO, 295 K) of the oxidation of MPS using 1 mol% **4c** as the photosensitizer

Table S4 Photooxidation of MPS by using different porphyrin photosensitizers

Photosensitizer	Conversion (%)	Yield (%)[a]	TOF (min^{-1})	Time (min)
1	74.3	50.0	0.36	140
4a	88.1	61.8	0.44	140
4b	85.9	59.6	0.43	140
4c	94.4	70.4	0.50	140

Reaction conditions: substrate (26 μmol), photosensitizer (1 mol%), DMSO (2 mL), room temperature, O_2 atmosphere. Samples were irradiated with a light-emitting diode (LED) lamp (λ_{ex} = 405 nm, 4.36 W).

[a]Crude yields determined from ^{1}H NMR based on the starting material with internal standard mesitylene.

References

[S1] D. Schaming, Y. Xia, R. Thouvenot and L. Ruhlmann, *Chem. Eur. J.*, 2013, **19**, 1712—1719.